Waste Tire Pyrolysis and Distillation for Designing Effective Asphalt Rejuvenators

José R. Colina[a], Manuel Chavez-Delgado[b,c], Claudio Álvarez[d], Cristina Segura[e], Rodrigo Delgadillo[f], Jose L. Concha[b], Luis E. Arteaga-Pérez[g*] Jose Norambuena-Contreras[h*]

[a]*Facultad de Ciencias, Universidad San Sebastián, Lientur 1457, Concepción 4080871, Chile*

[b]*LabMAT, Departamento de Ingeniería Civil y Ambiental, Universidad del Bío-Bío, Concepción, 4051381, Chile*

[c]*Departamento de Ingeniería Civil, Facultad de Ingeniería, Sede Concepción 4300866, Universidad Andres Bello, Chile*

[d]*Laboratory of Thermal and Catalytic Processes (LPTC), Department of Process Engineering and Bioproducts, Engineering Faculty, Universidad del Bío-Bío, Concepción, 4030000, Chile*

[e]*Unidad de Desarrollo Tecnológico, Universidad de Concepción, Coronel, Chile.*

[f]*Departamento de Obras Civiles, Universidad Técnica Federico Santa María, Valparaíso 2390123, Chile*

[g]*Department of Chemical Engineering, Faculty of Engineering, Universidad de Concepcion, Chile*

[h]*Advanced Bituminous Materials Laboratory, Department of Civil Engineering, Faculty of Science and Engineering, Swansea University, SA1 8EN, United Kingdom*

*Corresponding authors: larteaga@udec.cl; j.norambuena@swansea.ac.uk

ABSTRACT

The pyrolysis of waste tires presents a sustainable strategy to convert polymeric waste into functional pyro-oil asphalt rejuvenators. However, the chemical complexity and variability of pyro-oils have hindered consistent performance and predictive control. In this study, we develop optimized pyro-rejuvenators (PRs) aimed at restoring the self-healing properties of aged asphalt binders. Employing response surface methodology (RSM), we determined ideal pyrolysis conditions for producing PRs from Passenger Car Waste Tires (PCWT) and Haul Truck Waste Tires (HTWT). The optimum PRs were obtained from the 160–200 °C distillation fractions of pyro-oils produced at pyrolysis temperatures of 450 °C (PCWT) and 470 °C (HTWT). These rejuvenators feature a high content (>95%) of monoaromatics and alkenes coupled with low viscosity (<10 cP). Notably, PRs derived from PCWT and HTWT enhanced the healing index of aged bitumen by 26.6% and 45.3%, respectively, compared to natural recovery. This performance improvement strongly correlates with the limonene and cymene concentrations in the PRs. These findings advance the development of pyro-rejuvenators that not only restore the self-healing capacity of asphalt binders but also demonstrate the promise of sustainable tire-derived additives as key enablers of a circular economy.

Keywords: Waste tires; Pyrolysis; Distillation; Self-healing asphalt

1. INTRODUCTION

The rapid growth of the global population and rising living standards have significantly boosted the demand for connectivity. Annual passenger traffic is projected to increase by 50% by 2030, reaching 80 trillion passenger-kilometers [1]. The operation of existing roads and construction of new ones are expected to grow to meet rising demands. Around 90% of paved roads worldwide are made with asphalt mixtures [2,3]. Asphalt mixtures are subjected to environmental conditions and traffic loads throughout their service life, leading to both physical and chemical deterioration. This degradation compromises functionality and consequently increases the

requirements for maintenance, rehabilitation, or replacement [4,5].

An asphalt mixture typically comprises aggregates, bitumen, and air voids. Bitumen serves as the binder, imparting strength, flexibility, and durability to the pavement [6]. Bitumen is a complex viscoelastic material made of organic compounds (saturates, aromatics, resins, and asphaltenes) derived from petroleum refining. Due to its composition and exposure to environmental conditions, bitumen suffers aging [7]. Aging is an oxidative process that modifies the composition and properties of bitumen, resulting in increased stiffness and brittleness. This makes the asphalt mixture more susceptible to distress and is a primary factor contributing to asphalt pavement deterioration [8,9].

Numerous studies have investigated the use of rejuvenating agents to restore the rheological, mechanical, and chemical properties of aged asphalt binders [5,10–14]. Rejuvenators are low-viscosity oils with aromatic and maltene-like compounds, capable of replenishing the chemical species lost during aging. Rejuvenators also improve the solubility between bituminous fractions and enhance the colloidal stability of asphalt binders [15]. Asphalt rejuvenating agents can be classified into two primary categories: petroleum-based and non-petroleum-based rejuvenators [16]. The latter group has attracted attention in recent years because they can be produced from industrial wastes [16,17] or biomass [18,19], which makes them an economical and sustainable alternative to the petroleum-based rejuvenators. Among the residues used as precursors for asphalt rejuvenators, waste tires offer distinct advantages due to their abundance and their potential to be converted into functional additives through pyrolysis [20–24].

Norambuena-Contreras et al. [25], were the first to demonstrate that the liquid fraction (pyro-oil) obtained from the pyrolysis of waste tires can diffuse into aged asphalt binder, promoting its self-healing. This effect was due to the low viscosity and chemical composition of the pyro-oil. The authors suggested that aromatics and alkenes effectively induce self-healing by replenishing the maltene fraction in aged asphalt binders. In the same line, Li et al. [26] attributed

the rejuvenating potential of bio-oil from co-pyrolysis of wood and waste tire rubber to its high content of aromatic and olefinic compounds. The rejuvenating effectiveness of pyro-oils from waste tires is driven by their physical characteristics and the presence of critical chemical constituents like aromatics and alkenes. Nonetheless, precisely controlling pyro-oil composition is highly challenging and necessitates advanced upgrading techniques, including thermal cracking, catalytic hydrotreating, and distillation.

A recent work by Campuzano et al. [27] confirmed that the pyro-oils from waste tires can be fractionated by distillation at atmospheric conditions into four different cuts, namely light (70 – 176 ºC), low-middle (176 – 240 ºC), high-middle (240 – 285 ºC) and heavy (285 – 550 ºC). The physicochemical characterization showed that distillation cuts from 70 to 285 ºC mainly contained light aromatic (mono- and di-aromatics) and aliphatic compounds, while the heavier fractions were highly viscous due to the presence of polycyclic aromatics and sulfur-containing species. These authors focused on the structural characterization of the liquids, aiming to explore their potential use in refinery processes to produce fuels of varying qualities. A key finding of Campuzano's work is that the distillation cuts of pyro-oils vary depending on the type of waste tire and the specific pyrolysis conditions employed. Therefore, any intended application of these pyro-oils should be preceded by a comprehensive analysis of the waste tire composition, as well as the pyrolysis and distillation parameters.

Chavez-Delgado et al. [11] performed pioneering work on the synthesis of a pyro-rejuvenator derived from the pyrolysis of waste tire blends, combining 50/50 weight ratio of rubber fractions from light vehicles and mining trucks. In this study, they demonstrated that the effectiveness of pyro-rejuvenator should be controlled by adjusting the reaction temperature during pyrolysis and by further distilling the crude TPO into aromatics and terpene´s rich fractions. More recently, the same research group have reported that pyro-rejuvenators could enhance the rheological and self-healing properties of aged bitumen. Their results suggest that

specific chemical species such as aromatics and terpenes, are active for inducing self-healing, while heavier molecules like PAHs are detrimental [28].

Despite extensive research on waste tire pyrolysis and pyro-oil upgrading, limited understanding remains regarding the influence of reaction conditions, waste tire composition, and distillation on the effectiveness of pyro-rejuvenators for asphalt applications. While certain aromatics and alkenes possess rejuvenating properties, light fractions may volatilize during asphalt preparation, reducing their efficacy. Therefore, a thorough analysis of waste tire pyrolysis combined with tandem distillation is critical for optimizing the chemical composition of pyro-rejuvenators. While most studies on pyro-oils as asphalt rejuvenators focus on their chemical effects, comparatively little attention has been given to the mechanical performance of the restored asphalt.

This study introduces a novel approach for developing asphalt rejuvenators using upgraded pyrolytic oils derived from passenger car waste tires (PCWT) and haul truck waste tires (HTWT). The innovation lies in optimizing the yields of key chemical families (particularly aromatics and alkenes) through an integrated pyrolysis–distillation process guided by response surface methodology (RSM). A systematic analysis establishes clear correlations between the chemical composition of pyro-oils and their ability to restore the self-healing capacity of aged bitumen. By precisely controlling the chemical profiles of pyro-oils from both PCWT and HTWT, this method offers a pathway to designing more effective asphalt rejuvenators. Importantly, it provides a sustainable route to valorize challenging waste streams while simultaneously extending the service life of asphalt pavements, addressing both environmental and infrastructure performance challenges.

2. MATERIALS AND METHODS

2.1. Materials

The polymeric fraction from Passenger Car Waste Tires (PCWT) and Haul Truck Waste Tires

(HTWT) was used as feedstock for the pyrolysis experiments. These materials were supplied by local companies as granules (free of steel and textiles) with particle sizes ranging from 1 to 2 mm. Virgin bitumen with a penetration grade of 50/70 (density 1.04 $g \cdot cm^{-3}$ at 25 ºC, softening point 50 ºC, viscosity 900 mPa.s at 60 ºC) was used for asphalt healing tests. Before healing, the bitumen was subjected to short-term and long-term simulated aging by following the ASTM D 2872-22 [29] and ASTM D 6521-22 [30] standards, respectively.

2.2. Characterization of waste tires

The PCWT and HTWT were characterized for their elemental composition in a Leco CHNS 628 elemental analyzer following the ASTM D529 standard [31], while the proximate analyses were performed in a muffle furnace (Thermo Scientific F6020C) according to the ASTM D3172 standard [32]. Additionally, inorganic elements were quantified using inductively coupled plasma optical emission spectrometry (ICP-OES) in a PerkinElmer Optima 7000 DV ICP-OES. Thermogravimetric analysis (TGA) was conducted using a Netzsch STA 409PC device. The analysis was performed from room temperature to 600 ºC at a heating rate of 10 $ºC.min^{-1}$ under a N_2 atmosphere (50 $mL.min^{-1}$).

2.3. Production of pyro-oils

The pyrolysis of the PCWT and HTWT was carried out in a custom-designed laboratory setup (Fig. 1). The testing rig included a cylindrical fixed-bed reactor (ID:128 mm and H:235 mm) equipped with a mechanical stirrer. The reaction temperature (400<T<500 ºC) was monitored using six K-type thermocouples placed along the reactor, while the automatic control was programmed to keep a uniform thermal profile within the reaction chamber. In a typical experiment, 400 g of waste tires were pyrolyzed by 120 min under flowing N_2 (1 $L \cdot min^{-1}$). The pyro-oil was obtained after two consecutive stainless water-cooled condensers (ca. 15 ºC) installed downstream the reactor. Non-condensable gases were washed and safely released into the atmosphere through flaring. The solid product, known as recovered carbon black, was

collected from the reactor after cooling to room temperature. All experiments were performed in duplicate to ensure reproducibility.

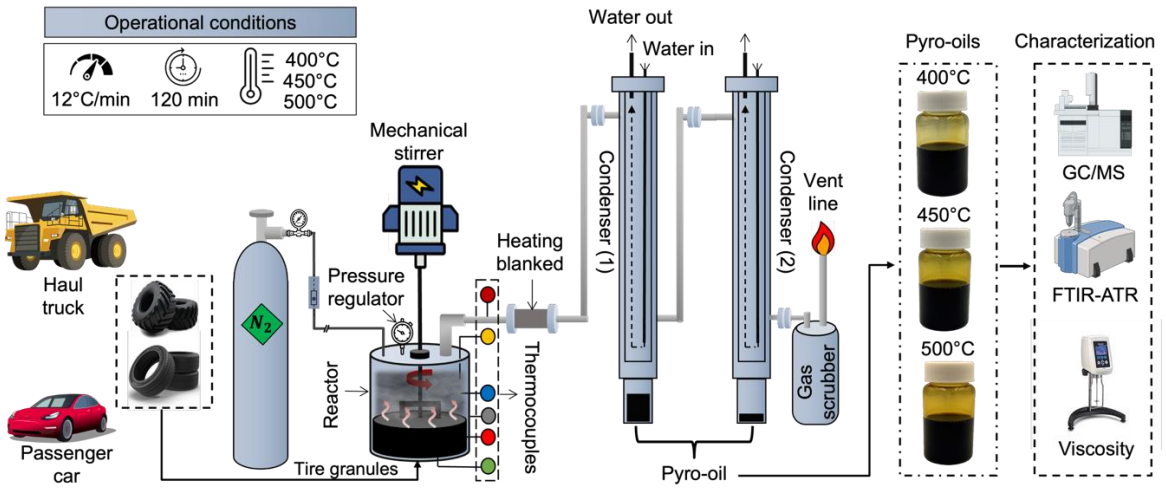

Figure 1. Experimental set-up for production of pyro-oils from PCWT and HTWT materials. 400 °C < T < 500 °C, 400 g/batch, stirrer (500 rpm), 12 °C·min^{-1} heating ramp, 120 min of pyrolysis time and condensation at 15 °C.

2.4. Upgrading of pyro-oils as asphalt rejuvenators

The potential of pyro-oils as asphalt rejuvenators is closely linked to their physical properties and chemical composition. To explore this potential, the pyro-oils underwent physicochemical upgrading through conventional distillation, following a procedure similar to that reported by Campuzano et al. [27] and show in Figure 2. Briefly, distillation curves at atmospheric pressure were obtained for pyro-oils produced from PCWT and HTWT following the ASTM D 86 standard [33]. For the distillation, 200 mL of pyro-oil were placed in a round-bottomed flask equipped with a mechanical stirrer (200 rpm). The liquid was gradually heated from room temperature (15 ºC) to 280 ºC using a heating mantle. Temperature control was achieved with two K-type thermocouples, one inside the distillation mixture and the other at the vapor outlet. As the temperature increased, condensed vapors were collected, and distillate volume fractions were recorded as a function of temperature. The distillation curves were arbitrarily divided into

five cuts: i) <160 ºC, ii) 160 ºC–200 ºC, iii) 200 ºC–250 ºC, iv) 250 ºC–280 ºC, and v) >280 ºC. Each cut was then characterized to inspect its physical properties and chemical composition.

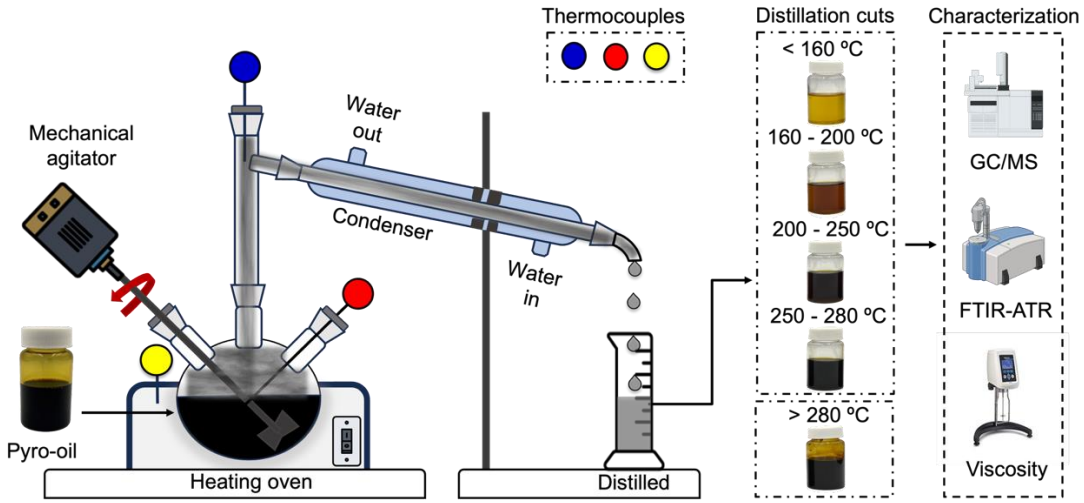

Figure 2. Experimental set-up for distillation of pyro-oils obtained from PCWT and HTWT materials. Room temperature < T < 280 °C, 200 mL/batch, stirrer (200 rpm).

Furthermore, the distribution of products was qualitatively evaluated using the chromatographic area-selectivity criterion (S) for all chemical species identified in the GC/MS analysis of the pyro-oils (Eq. 1) [34]. Additionally, a semi-quantitative assessment of rejuvenating active species (aromatics and alkenes) was conducted to determine their yields in the distillation cuts, as defined in Eq. 2:

$$S_{C-i} = \left(\frac{GCA_{i-comp}}{\sum_{i=1}^{n} GCA_{i-comp}}\right) \quad (1)$$

$$Y_{C-i,j} = (Y_{Oil}) * (Y_{cut}) * (X_{C-i}) \quad (2)$$

where: $Y_{C\text{-}i,j}$ is the mass yield of the (i) compound within the (j) family (j = aromatics, alkenes) in the distillation cut per kg of pyrolyzed tire ($g_i \cdot kg_{WT}^{-1}$), Y_{Oil} is the yield of the oil from pyrolysis ($kg_{oil} \cdot kg_{wt}^{-1}$), Y_{cut} is the yield of the distillation cut ($g_{cut} \cdot g_{oil}^{-1}$), and $X_{C\text{-}i}$ is the mass fraction of compound (i) in the distillation cut ($g_i \cdot g_{cut}^{-1}$) obtained for each "target" compound

(aromatic and alkenes). $GCA_{i\text{-}comp}$ is the peak area of the gas chromatogram for the *i-th* component in the pyro-oil and $S_{C\text{-}i}$ is the area-selectivity for each component.

2.5. Physical and chemical characterization of pyro-oil and distillation cuts

Chemical composition of crude pyro-oils and its distillation cuts were analyzed by Fourier transformed infrared spectroscopy (FTIR) and gas chromatography/mass spectrometry (GC/MS). The FTIR analysis was carried out using a Nicolet is20 (Thermo Fisher, USA) spectrometer equipped with a total attenuated reflection accessory (Specac Golden Gate ATR, UK). The sample spectra were averaged from 32 scans with a resolution of 4 cm^{-1} over the mid-IR range (4000–600 cm^{-1}). All the spectra were normalized before analysis to avoid any *bias* in the further interpretation of the results. The intense signal at 2917 cm^{-1} was taken as the basis for such normalization [35].

GC/MS analysis was performed using a GC–2010 Plus gas chromatograph (Shimadzu) coupled with an Ultra single quadrupole mass spectrometer (QP 2010, Shimadzu). In a standard analysis, 0.02 g of pyro-oil was diluted in 1 mL of analytical-grade acetone, and 1 µL of the mixture was injected into the GC through a split/splitless port preheated to 250 °C with a 1:100 split ratio. Helium (99.999%) was utilized as the carrier gas at a flow rate of 1.04 $mL.min^{-1}$. The compounds were separated using a 60 m ZB-5ms capillary column (0.25 µm x 0.25 mm) and further eluted following this temperature program: 40 °C with a dwell time of 1 min, a ramp of 5°C.min^{-1} to 180 °C with a dwell time of 2 min, and a subsequent ramp of 15°C.min^{-1} to 280 °C with a dwell time of 20 min. The MS source was maintained at 250 ºC, with the interface set to 280 ºC, and the analysis conducted in SCAN mode over the range of 35 – 550 m/z. The ion mass spectra were analyzed in comparison to the NIST database for the purpose of compound identification. The GC results were correlated through Eq. 1 to estimate the area-selectivity for each pyro-oil [34].

In addition to the qualitative GC/MS analysis, aromatics and alkenes were quantified to determine their specific yields (Eq. 2). To that aim, external calibration curves for representative compounds (i.e., toluene and cymene for aromatics and limonene for alkenes) were constructed to obtain experimental response factors (RFs) under identical chromatographic conditions (R^2 > 0.99; Figs. S1-S3). Concentrations of the remaining species within each family were estimated using the Effective Carbon Number (ECN) approach adapted by Kim et al., [36,37] for GC/MS. The ECN was determined as the sum of the carbon number equivalent (CNE) for each selected molecular descriptor multiplied by its number of occurrences within the molecule (Eq. 3). Initially, the molecular descriptors were chosen to include three atoms (C, H, O), and a functional group: (–OH), which for a Q-MS detector is correlated as follows:

$$ECN_i = \sum_{C=1}^{n}(C) + 0.24 * \sum_{H=1}^{m}(H) - 0.70 * \sum_{H=1}^{m}(O) + 0.55 * \sum_{-OH=1}^{p}(-OH) \quad (3)$$

Then the concentration of each compound was calculated as follows:

$$C_i = \left(\frac{A_i}{RF_{ref}}\right) * \left(\frac{ECN_{ref}}{ECN_i}\right) \quad (4)$$

here A_i is the peak area of analyte i, RF_{ref} is the response factor of the reference compound within the family (toluene for aromatics; limonene for alkenes), and ECN_i and ECN_{ref} are the corresponding effective carbon numbers. A detailed list of the analytes considered for quantification along with their ECN, RF and concentrations is provided in the Supplementary Material (Tables S1 and S2).

Finally, key physical properties for asphalt healing applications were analyzed in pyro-oils and distillation cuts. Water content was measured by Karl-Fisher titration (Mettler Toledo, V20), viscosity was determined using a rotational viscometer (Fungilab, Smart series) at 20 ºC per ASTM D445, and pH (Tecnal TEC-7) and density were also assessed.

2.6. Fine-tuning of pyro-rejuvenator composition

The optimization of the pyro-rejuvenator composition was carried out by a 3^k central composite design (CCD). The CCD considered pyrolysis conditions and distillation cuts as main variables,

with the yield of aromatics and alkenes as the effectiveness criteria (response variables). The factors included in the design and the operating range of the variables are shown in Table 1. These ranges were defined inspired in previous literature reports [11,16,38–41]. The experimental data were analyzed using ANOVA, and Response Surface Methodology (RSM) identified the optimal operational conditions. Design Expert software, version 11 (Stat-Ease Inc., USA), was used for the analysis.

Table 1. Design of experiment (DOE) applied for the optimization to produce optimized pyro-rejuvenators from PCWT and HTWT pyrolysis.

Factor	**Factor type**	**Low level (-)**	**Central point (0)**	**High level (+)**
Pyrolysis temperature (ºC)	Variable	400	450	500
Distillation cut (ºC)	Variable	160-200	200-250	250-280
Raw material (g)	Variable	400	400	400
Heating rate (ºC·min^{-1})	Constant	12	12	12
Pyrolysis time (min)	Constant	120	120	120
Aromatics yield (g·kg$_{wt}^{-1}$)	Response			
Alkenes yield (g·kg$_{wt}^{-1}$)	Response			

2.7. Self-healing test for validating pyro-rejuvenator activity

The effect of optimized pyro-rejuvenators on the self-healing properties of long-term aged bitumen (using PAV-aged process [30]) was assessed to validate the correlation between chemical optimization conditions and mechanical performance of treated bitumen. To that aim, aged bitumen samples were evaluated under the tensile strength recovery of crack-healing test samples before and after a 24-hour healing period, according to the method proposed by Chavez-Delgado et al. [23]. The assays involved a three-step method, as described below and shown in Figure 3:

Step 1. Conditioning process: PAV-aged ductility samples were prepared and conditioned at -5 °C for 2 h in a freezer, see Figure 3a.

Step 2. Crack generation and application of pyro-rejuvenator: The PAV-aged ductility samples were tensile tested at a rate of 5 mm/min at 5 °C until the sample broke into two pieces with flat fracture surfaces. Then, 3 μL of the optimized PCWT and HTWT pyro-rejuvenators were applied to each fracture surface using a micropipette and evenly spread with a laboratory spatula. To avoid interference of mass transfer due to different diffusional behavior, this treatment was carried out under strict temperature control (20 ºC) (Fig. 3b).

Step 3. Healing process: Next, the two pieces were carefully reassembled in the ductility mold. To avoid inducing healing through pressure, they were fixed in place using two socket head cap screws, as shown in Figure 3c. The samples were then kept at ambient temperature (20 °C) for 24 hours to ensure sample integrity for subsequent testing. After the healing period, the sample was removed from the mold and tested again under tensile testing (step 1), completing one fracture-healing-fracture cycle. From this, a Healing Index (HI) was determined using the equation 5:

$$HI\ (\%) = \left(\frac{F_h}{F_i}\right) \times 100 \quad (5)$$

where F_i and F_h are the maximum forces resisted by the sample before and after the healing process, respectively.

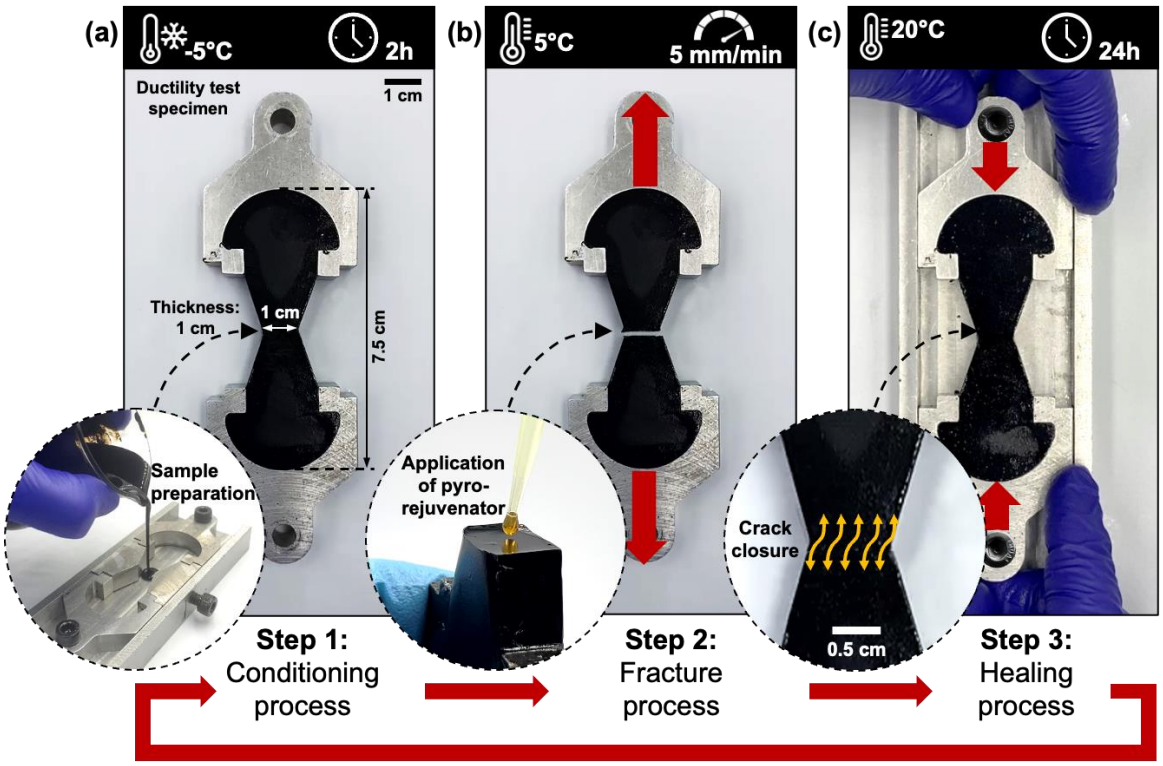

Figure 3. Self-healing process of PAV-aged bitumen sample under tensile test using ductility test specimens (ASTM D 113 – 17 [42], illustrating the steps of a) conditioning, b) fracture, and c) healing processes. Figure adapted with permission from [23], Copyright [2025] [Elsevier].

3. RESULTS AND DISCUSSION

3.1. Characterization of waste tires

Both waste tires had similar volatile matter and moisture contents; however, PCWT had higher fixed carbon and lower ash contents than HTWT (Table 2). Fixed carbon (non-volatile) in the tires primarily comes from carbon black, while the ash represents the inorganic materials in the tires [43,44]. Elemental analysis confirmed the high carbon content in these wastes, which, together with their volatile matter, supports their suitability as feedstock for pyrolysis. The quantification of inorganic elements revealed low proportions of iron, calcium, zinc, aluminum, silicon, potassium, and sodium in both waste tires. The presence of iron is mainly attributed to particles from steel wire remaining after tire pre-treatment, while the other inorganics likely originated from additives in the tires [45]. Although the metallic elements detected in the raw material could

have a catalytic effect, their low concentrations (in the ppm range) suggest they play a minimal role in the pyrolysis reactions [43,46].

Table 2. Compositional analysis of PCWT and HTWT waste tires.

Proximate composition			**Elemental composition**					
	(wt.%)			(wt.%) $_{d.b}$			(mg kg^{-1}) $_{d.b}$	
	PCWT	HTWT		PCWT	HTWT		PCWT	HTWT
Moisture	1.27	0.99	C	80.4	76.5	Fe	4163	3170
Volatile matter	65.5	67.2	H	7.1	7.1	Ca	2687	2042
Fixed carbon	24.98	18.71	N	0.52	0.40	Zn	1121	1061
Ash	8.25	13.1	S	2.2	1.5	Al	955	838
			O*	1.6	1.3	Si	822	730

d.b: results are reported in dry base.

* Oxygen was determined by the difference from C, H, N, S, and ash.

The thermal degradation of PCWT and HTWT shows four major stages, labeled S1 to S4 in Figures 4a and 4b. In PCWT, the first stage (S1) occurs between 185 and 330 ºC, while in HTWT, the decomposition begins at 220 ºC. This initial mass loss is attributed to the volatilization of plasticizers and other additives from the tires, as well as the initiation of unzipping reactions in natural rubber (polyisoprene) [47,48]. The weight loss in this primary stage ranged from 3 to 5%, with a higher loss observed for PCWT, suggesting a greater proportion of additives in these samples.

The second and more significant mass loss (S2) occurred in the temperature range of 330–410 ºC for both samples, accounting for 31–39% of the total mass loss. This thermal event is primarily associated with the depolymerization of natural rubber (NR) [49], although partial conversion of synthetic rubbers could also take place. It has been proposed that the degradation of NR, butadiene rubber (BR) and styrene butadiene rubber (SBR) occurs via two consecutive devolatilization reactions (primary and secondary devolatilization) at increasing temperature.

Primary devolatilization, occurring at lower temperatures for NR, involves the formation of radicals that depolymerize into volatile monomers and/or dimers or recombine to form intermediate condensed products. During secondary devolatilization, these condensed products are further degraded through fragmentation and other rearrangements, including aromatization and crosslinking [50,51].

In stage S2, the higher and sharper peak observed in the DTG curve of HTWT indicates a more accelerated devolatilization in this temperature range, likely due to a higher NR content compared to PCWT. In fact, it has been reported that truck tires have a higher proportion of NR compared to passenger car tires, which may be attributed to the higher mechanical standards required for truck tires in the mining industry [50,52].

Additionally, stage S3, extending from 410 ºC to about 500 ºC, is characterized by a shoulder-like peak in the DTG curve and is attributed to secondary devolatilization reactions, mainly of synthetic rubbers. This stage is wider and sharper for PCWT, confirming that the BR and SBR contents in these tires are higher than in HTWT [51].

Finally, a fourth stage (S4) above 500 ºC is associated with secondary and tertiary reactions, including crosslinking and carbonization, which result in recovered carbon black and ash [53]. This is supported by the similarity in the solid residue remaining at 500 ºC, which matches the fixed carbon and ash contents recorded during the proximate analysis.

The TGA results show that at 500 ºC, all raw materials have depolymerized, and no additional thermal events occur. However, in addition to temperature, the heating rate and vapor residence time should be carefully controlled to optimize the pyro-oil composition.

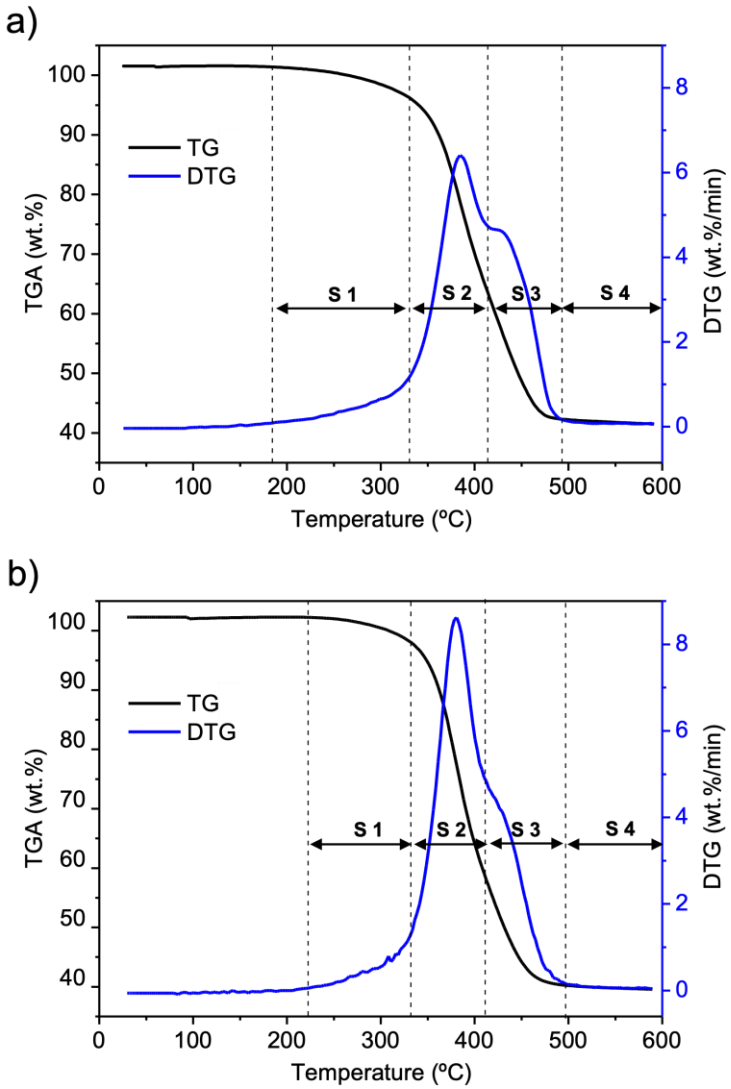

Figure 4. TG and DTG curves of waste tires samples. a) PCWT and b) HTWT. Dashed black lines separate the mass loss stages.

3.2. Mass balance of waste tires pyrolysis

The TGA analysis (Fig. 4) showed that the thermal decomposition of the rubber in both types of tires began around 330 ºC and ended at approximately 500 ºC. An exploratory pyrolysis experiment at 350 ºC was conducted before carrying out the full experimental design outlined in Table 1. This experiment resulted in an incomplete conversion of the tires, with the solid product being a sticky, gummy heterogeneous mixture, and a yield greater than 70 wt.%.

Conversely, operating at temperatures above 500 ºC favors the production of the gas fraction at the expense of the liquid fraction, thereby reducing the yield of self-healing active compounds such as limonene [40,44,54]. Accordingly, the temperature range for the pyrolysis experiments was studied between 400 ºC and 500 ºC. Figure 5 shows a sharp increase in oil yield from 400 ºC to 450 ºC in both types of tires.

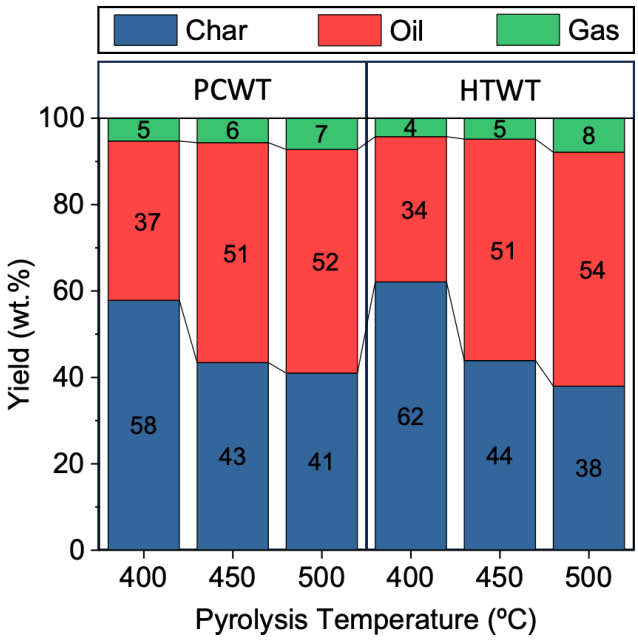

Figure 5. The yield (wt.%) of products obtained (char, oil and gas) from the pyrolysis of PCWT and HTWT at different temperatures.

The increase was approximately 15% for both tire types, suggesting that the depolymerization of natural and, to some extent, synthetic rubbers occur via similar reaction routes (unzipping, homolytic ruptures, and intramolecular cyclization). The pyro-oil yield stabilizes between 450 ºC and 500 ºC, and it was in the same order for both PCTW and HTWT (51 – 54 %). These results indicate that the conversion of the solid fraction through primary reactions occurred up to 450 ºC, while at higher temperatures, secondary reactions in the gas phase are favored [55]. This hypothesis is substantiated by the increase in the gas yield and the reduction in the recovered carbon black at 500 ºC [40,56]. The previous results suggest that the major differences

in the pyro-oils from PCWT and HTWT may lie in their composition, rather than in bulk yields, which were similar to those previously reported for other tire residues [57–59].

3.3. Chemical and physical characterization of pyro-oils

3.3.1. FTIR analysis

The pyro-oils obtained from PCWT and HTWT were analyzed by FTIR to identify the main functional groups. Figures 6a to 6e show the FTIR spectra of the oils obtained from PCWT and HTWT pyrolysis at 450 °C, with a zoom on regions corresponding to the most intense signals. In general, a slight effect of temperature and a significant influence of tire type on the functional groups detected by FTIR were observed.

The strong absorption bands observed between 3000 – 2800 cm^{-1} and 1500 – 1350 cm^{-1} correspond to the C-H stretching and deformation vibrations in alkanes, which were present in oils from both waste tires (Fig. 6b). Moreover, the peaks between 830-980 cm^{-1} and 1680-1620 cm^{-1} can be ascribed to the C=C stretching vibrations in alkenes and cycloalkenes units. In this region, the signal at 886 cm^{-1} ascribed to alkenes was more intense for HTWT than for PCWT (Fig. 6c). This may be due to an increased presence of limonene, which is derived from polyisoprene, a rubber predominantly found in HTWT. In contrast, the presence of aromatics in both oils was confirmed by the vibration bands at 1120 – 1000 cm^{-1} and 780 – 675 cm^{-1}. Finally, the broad peak observed from 3700 cm^{-1} to 3100 cm^{-1} was assigned to stretching vibrations of the O-H group, evidencing the existence of hydroxylated compounds such as alcohols, phenols or acids in oils, which were classified as others (Fig. 6e). The attribution of the absorption bands was inspired by previous reports [49,56,60].

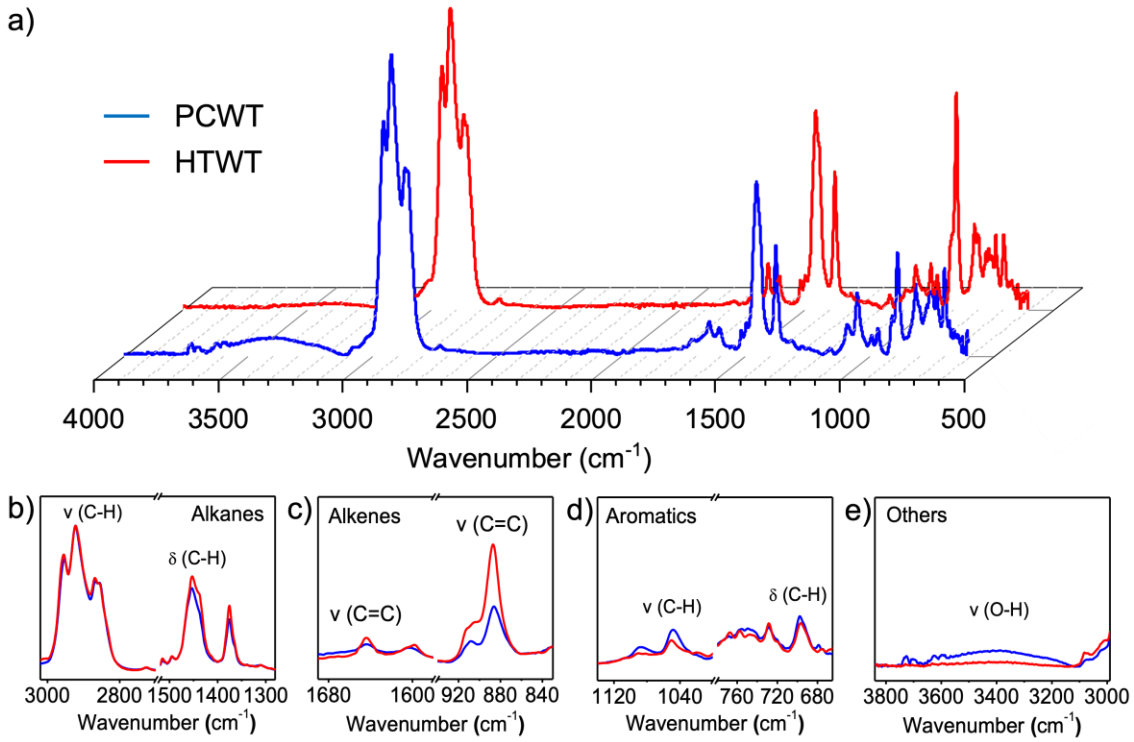

Figure 6. FTIR spectra of oils obtained from the pyrolysis of PCWT and HTWT at 450 ºC. a) complete Mid-IR spectra; b-c) comparison of the intensities of the absorption bands assigned to alkanes, alkenes, aromatics and others, respectively.

The FTIR analysis results show that pyro-oils mainly contain aliphatic and aromatic compounds. These findings are comparable to those reported by other authors [61,62]. To identify the main chemical compounds and correlate their nature with the rejuvenating potential of the oils, a GC/MS analysis was conducted.

3.3.2. GC/MS analysis

Figure 7 shows the GC area-related selectivity of pyro-oils obtained from HTWT and PCWT. A complete list of the identified compounds along with their selectivity (Eq. 1) is provided in Table S3. The oils obtained from PCWT exhibit a higher abundance of monoaromatics compared to those from HTWT, which mainly contain aliphatic compounds, with nearly 80% of them being alkenes. It has been demonstrated that aromatic compounds, particularly single ring aromatics such as toluene, xylene, styrene and other alkyl benzenes are mainly derived from the degradation of SBR or by cyclization of alkenes followed by hydrogenation and Diels-

Alders reactions [40,63]. On the other hand, aliphatic compounds such as alkenes are related to the primary degradation of NR (scissions and radicalizations) and secondary reactions starting from isoprene. Therefore, the concentrations of these functionalities in the pyro-oils heavily depend on the proportions of NR, BR, and SBR in the tires, as well as on the reaction temperatures [39,62]. Interestingly, limonene ($C_{10}H_{16}$), was the major compound identified in the pyro-oils, regardless of the type of waste tire. This cycloalkene is formed from two isoprene units through intramolecular cyclization of the allylic radicals produced by random polyisoprene chain scission [64,65]. Therefore, the presence of limonene is proportional to the NR content in the waste tires, which explains its higher concentration in the pyro-oils produced from HTWT (see Table S3).

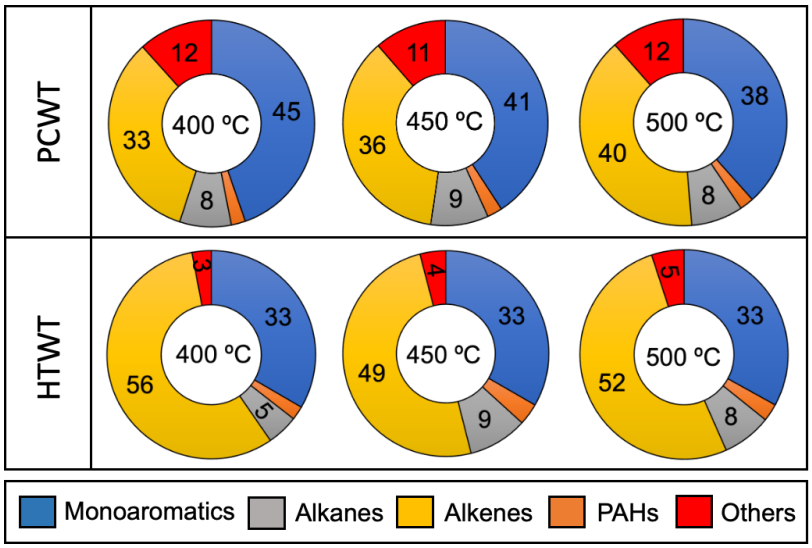

Figure 7. Product distribution represented as area-related selectivity (Eq. 1) for pyro-oils derived from PCWT and HTWT at different temperatures.

In addition to the valuable monoaromatics and aliphatic detected in the pyro-oils, other polycyclic aromatic hydrocarbons (PAHs), such as alkyl derivatives of naphthalene, were also identified. The presence of these PAHs is explained by the occurrence of Diels–Alder reactions involving the cyclization and dehydrogenation of alkenes [40,66]. The selectivity of compounds classified as "others" was significantly higher in the PCWT compared to the HTWT. This group included nitrogenous, sulfurous, and oxygenated compounds, which mainly originate from the

degradation of vulcanizing agents and additives added to the tires [67,68]. In conclusion, compositional analysis revealed that, regardless of the waste tire source, pyro-oils possess potential for use as additives in asphalt rejuvenators. However, upgrading is necessary to enhance the concentration of healing-active species, such as alkenes and monoaromatics.

3.3.3. Physical characterization

All the pyro-oils exhibit slightly basic pH (8.1-8.4), water contents < 5% wt., densities < 1000 kg/m^3 and viscosities < 10 cP. Similar results have been reported by other authors [11,60,69,70]. Table 3 shows that the viscosity and density values increased with pyrolysis temperature in the oils from both types of tires. Remarkably, the low viscosity (<10 cP) suggests that the pyro-oils could easily flow into the micro-cracks of aged asphalt binder, promoting its healing [71]. Overall, the physical properties of the pyro-oils confirm their potential as asphalt rejuvenators. Specifically, the low viscosity, density, and intrinsic ability to dissolve bitumen fractions through specific chemical species would give asphalts treated with pyro-oils exceptional self-healing capacities. Therefore, the following sections will discuss the fine-tuning of these crude pyro-oils into optimized pyro-rejuvenators.

Table 3. Physical properties of pyro-oils from PCWT and HTWT.

Physical properties	**Pyrolysis temperature**					
	PCWT			**HTWT**		
	400	**450**	**500**	**400**	**450**	**500**
pH	8.3	8.2	8.1	8.4	8.4	8.3
Water content (wt.%)	4.9	3.3	3.6	4.2	2.9	2.5
Viscosity@20 (cP)	9.1	9.5	9.9	4.2	5.2	9.2
Density@20 (kg·m^{-3})	852	862	864	832	852	860

3.4. Upgrading of pyro-oils into asphalt rejuvenators via distillation

Figure 8 presents the distillation curves (from room temperature to 280 ºC) and the corresponding yields of distillation cuts for pyro-oils derived from PCWT and HTWT at various pyrolysis temperatures. The distillation curves (Fig. 8a and 8b) exhibit similar initial boiling points, beginning between 50–60 ºC. Beyond this point, the change in slope indicates that volumetric yields are influenced by both the type of waste tire and the pyrolysis temperature. Pyro-oils from HTWT showed higher volumetric yields compared to those from PCWT. However, at elevated pyrolysis temperatures, a reduction in yield was observed across all pyro-oil samples.

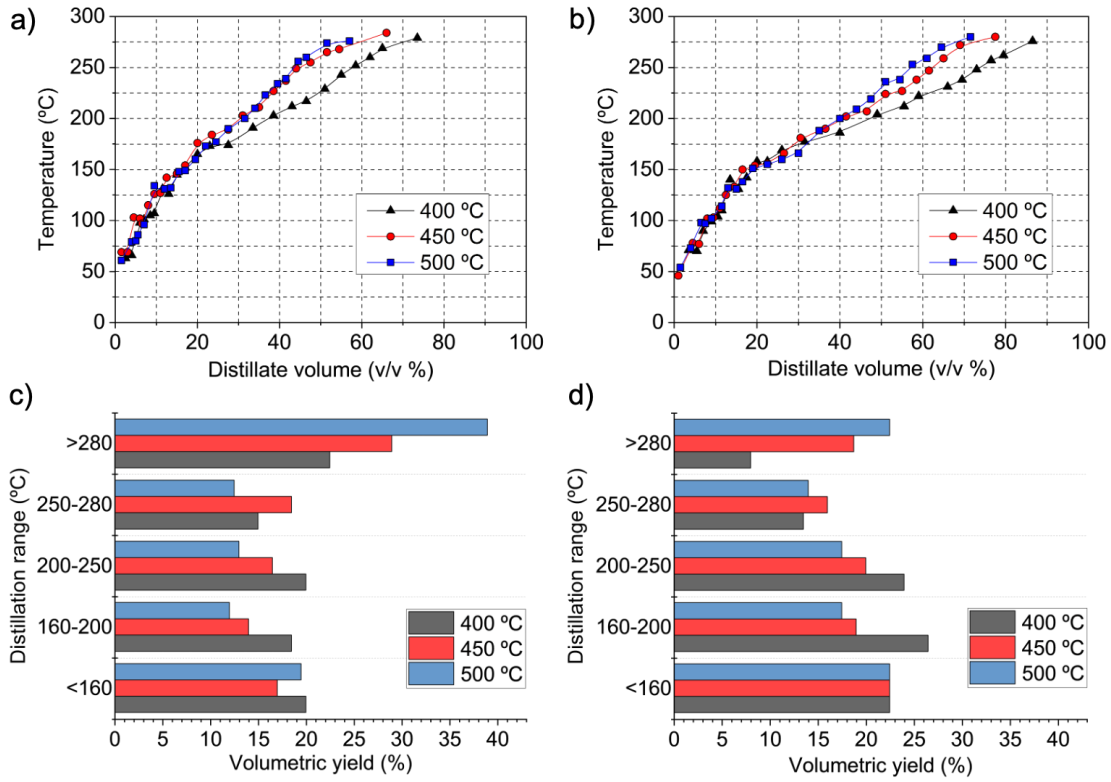

Figure 8. Separation of pyro-oils derived from waste tires. (a) Distillation curve of pyro-oil from PCWT; (b) distillation curve of pyro-oil from HTWT; (c) yields of distillation cuts from PCWT pyro-oil; and (d) yields of distillation cuts from HTWT pyro-oil.

In line with the distillation curves, Figures 8c and 8d show that in the cuts from <160 ºC to 250 – 280 ºC, the pyro-oils from HTWT exhibited higher yields. Conversely, the yield of liquids

remaining in the flask after the end of distillation (cuts >280 ºC), showed an inverse trend. These results indicate that an increase in pyrolysis temperature favors the formation of chemical compounds with higher boiling points, and these species are found in higher concentrations in the pyro-oils obtained from PCWT. In fact, GC/MS analysis (see Fig. 7) showed that the pyro-oils from PCWT had a higher relative abundance of polar heteroatom compounds (others), which have higher boiling points than hydrocarbons.

3.5. Chemical characterization of the distilled fractions

The distribution of chemical compounds identified in the distillation cuts is summarized in Figure 9. As shown, the cuts from PCWT (Fig. 9a) exhibited high selectivity to monoaromatics and heteroatomic compounds (categorized as "others"), whereas the cuts from HTWT (Fig. 9b) showed greater abundance of alkenes and polycyclic aromatic hydrocarbons (PAHs). Furthermore, as the distillation temperature increased, there was a noticeable rise in the presence of alkanes, PAHs, and other compounds, accompanied by a corresponding decrease in monoaromatics.

The cuts < 160 ºC consist almost entirely of light monoaromatics and alkenes (> 98 %). In these cuts alkyl monoaromatics such as toluene, ethylbenzene, xylene and alkenes isomers ($C_{10}H_{18}$) were mostly found. The cuts 160 – 200 ºC from PCWT were mainly composed of monoaromatics, while those from HTWT higher presence of alkenes was identified. The main compounds found in these cuts were limonene and cymene. These compounds are valuable raw materials for the chemical industry, recognized for their potent solvent and antioxidant effect [72–74]. Moreover, the capacity of oils rich in these compounds to diffuse and restore aged bitumen has been demonstrated in a previous paper from our group [41].

In the 200 – 250 ºC distillation range of both waste tires, a higher presence of alkenes was found, particularly in the oils from HTWT. The main compounds present in this range were alkyl indenes, alkyl benzenes, and alkyl cyclohexenes. Finally, in the 250 – 280 ºC cuts, long-

chain alkanes were primarily identified, including hexadecane, heptadecane, and octadecane. These cuts also concentrated on other high molecular weight and polar compounds, such as heteroatomic compounds (others) and PAHs.

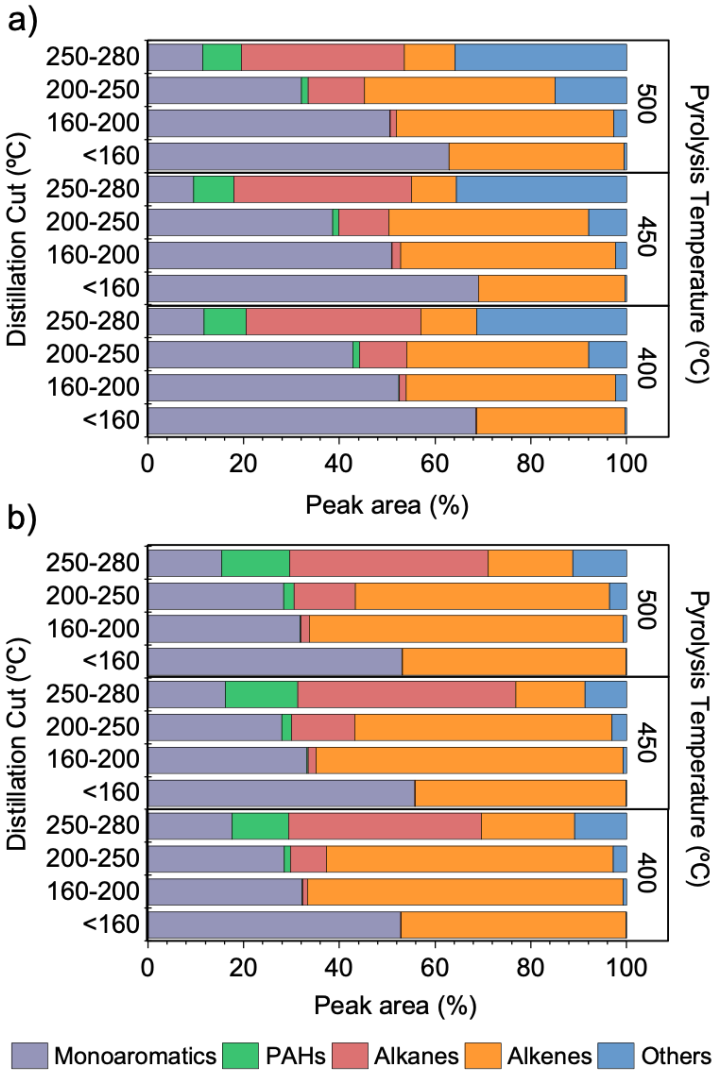

Figure 9. Chemical composition of pyro-oils distillation cuts from a) PCWT and b) HTWT.

The results of FTIR-ATR analysis for crude pyro-oils and their distillation fractions were consistent with GC/MS observations (Figures S4 and S5). After distillation, the proportion of compounds with rejuvenating activity (*i.e.,* monoaromatics and terpenes) was concentrated in fractions between 20 and 200 ºC. Meanwhile, other compounds like PAHs, remained in the heaviest fraction (>250 ºC). The observed product distribution was strongly influenced by the

type of tire from which they originate (Figs. S4 and S5). The results presented in this section demonstrate that distillation is an effective method to achieve a fine tuning of the pyro-rejuvenator composition. Notably, the high concentration of aromatics and alkenes presents in some cuts make them potential rejuvenators for asphalt self-healing. In addition, these cuts can also be used as substitutes for petroleum-based fuels and as potential sources of valuable compounds for the chemical industry, such as limonene, cymene and BTEX [53,75,76].

3.6. Optimization of pyro-oils as asphalt rejuvenators

The yield and composition of crude pyro-oils and distillation cuts indicate the need to control pyrolysis and distillation conditions to produce asphalt pyro-rejuvenators with enhanced self-healing properties. Self-healing capacity depends on the aromatics and alkenes content in the asphalt rejuvenators [16,25]. Thus, these species are fine-tuned using an RSM applied to a composite central design of experiment which includes the operational parameters of pyrolysis and distillation along with a semi-quantitative interpretation of chromatographic data (Table 1). The analysis focused on distillation cuts rich in aromatics and alkenes: 160–200 ºC, 200–250 ºC, and 250–280 ºC. Cuts below 160 ºC were excluded due to their evaporation at asphalt preparation and service temperatures [15]. Cuts above 280 ºC were excluded due to high viscosity (>50 cP) and elevated levels of PAHs and heteroatomic compounds, which could impair self-healing capacity [41]. The results of the experiments are reported as absolute mass yields for the target species as g per kg of waste tire ($g \cdot kg_{wt}^{-1}$) in Table 4.

Surface response plots in Figure 10 show the influence of pyrolysis and distillation temperatures on aromatic and alkene yields in distillation cuts. Figures 10a and 10b highlight that distillation temperature has a greater effect than pyrolysis temperature on the yields of target species from PCWT. The optimization model predicts maximum yields of both aromatics and alkenes (red zones) at distillation cut of 160–200 ºC and pyrolysis temperatures of 450 ºC. For HTWT pyro-oils (Figs. 10c and 10d), surface plots show that pyrolysis temperature strongly affects aromatic

yields, while distillation temperature primarily influences alkene yields. In agreement with the model, maximum yields of aromatics and alkenes in the HTWT pyro-oils were obtained at distillation cut of 160–200 ºC and pyrolysis temperatures of 470 ºC.

Table 4. Yield of aromatics and alkenes obtained from the pyrolysis and further distillation of pyro-oils from PCWT and HTWT.

Experiments		**PCWT**		**HTWT**	
Pyrolysis temperature (ºC)	Distillation cuts (ºC)	Aromatics yield ($g \cdot kg_{wt}^{-1}$)	Alkenes yield ($g \cdot kg_{wt}^{-1}$)	Aromatics yield ($g \cdot kg_{wt}^{-1}$)	Alkenes yield ($g \cdot kg_{wt}^{-1}$)
(-1) 400	(-1) 160-200	26.80	26.14	23.11	55.94
(0) 400	(0) 200-250	26.70	24.52	19.32	46.00
(+1) 400	(+1) 250-280	7.77	5.63	10.73	8.38
(-1) 450	(-1) 160-200	28.71	29.48	28.58	69.85
(0) 450	(0) 200-250	29.00	32.23	29.12	61.47
(+1) 450	(+1) 250-280	15.62	8.06	23.29	12.87
(-1) 500	(-1) 160-200	25.28	26.33	30.18	67.91
(0) 500	(0) 200-250	21.32	25.00	26.75	54.99
(+1) 500	(+1) 250-280	10.71	6.36	20.46	14.48

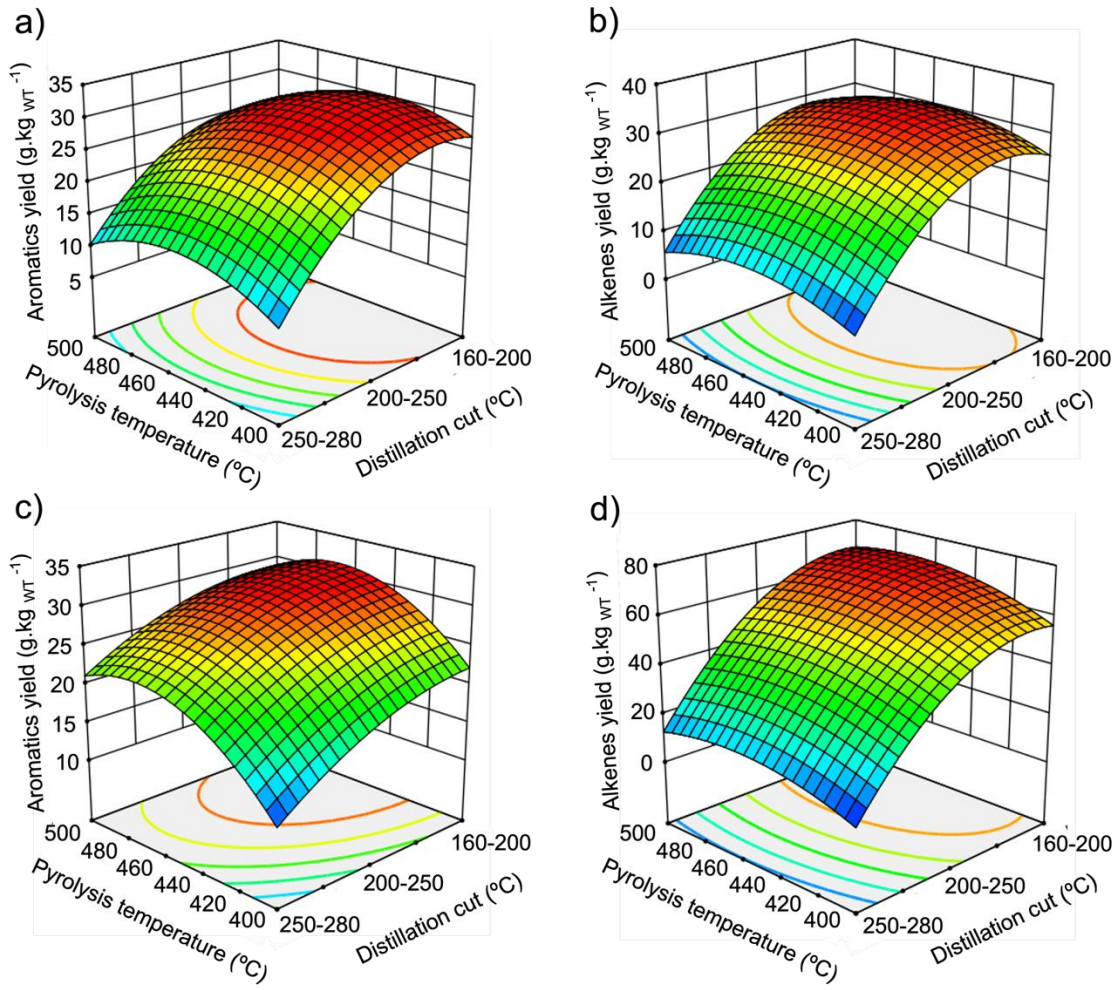

Figure 10. Graphs on the influence of pyrolysis and distillation temperature on the yield of aromatics and alkenes in the distillation cuts from a-b) PCWT and c-d) HTWT.

Pyro-rejuvenators were produced from HTWT and PCWT pyrolysis and further distillation under optimized conditions, and the yields obtained for aromatics and alkenes as well as physical properties are presented in Table 5. A comprehensive physicochemical characterization of both pyro-rejuvenators is available in the supplementary material (Table S4).

Table 5. Optimal conditions used to obtain the pyro-rejuvenators.

Optimal operation conditions			Pyro-rejuvenator yields			Pyro-rejuvenator properties	
Waste tire	Pyrolysis Temp. (°C)	Distillation Cut (°C)	Rejuvenator (g. kg_{wt}^{-1})	Aromatics (g. kg_{wt}^{-1})	Alkenes (g. kg_{wt}^{-1})	Viscosity (mPa.s)	Density ($g.cm^{-3}$)
PCWT	450 ± 2	160 – 200	51.94	25.69	34.14	1.72	0.84
HTWT	470 ± 2	160 – 200	94.19	48.27	58.76	1.70	0.80

Additionally, Table 6 presents the ANOVA results for the optimization model, highlighting the influence of process parameters (factors) and their interactions on aromatics and alkenes yields in the pyro-rejuvenators. The p-values for the models studied were statistically significant ($p < 0.05$) [77].

The distillation cuts significantly affected all response variables (p-value < 0.05). However, for PCWT, the p-values for temperature and its interaction with distillation cuts were above 0.05, suggesting the model is limited in describing and extrapolating data for this tire type. This behavior can be attributed to the higher content of additives, associated with compounds classified as "others" (Fig. 7), which are present in greater proportion in PCWT. These additives increase the compositional complexity of the feedstock and can influence the thermal decomposition pathways of the polymeric fraction, thereby diminishing the effect of temperature on the composition of the pyrolysis products [78]. Another factor contributing to the lack of statistical significance of temperature is the low variability observed in oil yields (1%) obtained between 450 and 500 °C (Fig. 5). This result suggests that near-complete devolatilization of the solid material was achieved at 450 °C. Further temperature increases cause only minor changes in oil yield, reflecting the predominance of secondary reactions. In contrast, the yields of aromatics ($p = 0.0160$) and alkenes ($p = 0.0424$) from HTWT are highly sensitive to pyrolysis temperature, due to the feedstock's elevated natural rubber (NR) content.

NR promotes the formation of limonene, which under specific thermal conditions generates intermediates such as terpinenes. These intermediates subsequently undergo dehydrogenation to form aromatics, providing a mechanistic explanation for the stronger temperature dependence observed in HTWT compared to PCWT.

Table 6. p-values from ANOVA for aromatics and alkenes yields in response to process parameters.

Source	PCWT		HTWT	
	Aromatics	**Alkenes**	**Aromatics**	**Alkenes**
Model	0.0197	0.0044	0.0262	0.0017
A-Pyrolysis Temperature	0.5463	0.7826	0.0160	0.0424
B-Distillation cut	0.0041	0.0009	0.0114	0.0003
AB	0.4185	0.8957	0.5550	0.4326
A^2	0.0692	0.0501	0.0345	0.0599
B^2	0.0305	0.0046	0.1981	0.0062

3.7. Validation of pyro-rejuvenator effectiveness in enhancing asphalt self-healing

The effectiveness of the optimized pyro-rejuvenators for inducing self-healing in aged bitumen was tested through a custom-designed experiment, adapted from Chavez-Delgado et al. [23]. Figure 11a shows the average compressive force results for PAV-aged bitumen samples before (reference line) and after being treated with pyro-rejuvenator. The assays were performed for optimal pyro-rejuvenators obtained from PCWT at 450 ºC (PCWT-450) and from HTWT at 470 ºC (HTWT-470). Overall, a reduction in tensile force was observed for the healed bitumen samples, with and without the addition of pyro-rejuvenators, compared to the reference PAV-aged bitumen (121.78 N). The tensile force values at rupture for the healed samples were 33.68 N for H-PAV (without pyro-rejuvenator), 66.13 N for H-PCWT-450, and 88.87 N for H-

HTWT-470. Thus, an improvement in recovering the initial tensile force was observed in samples with the pyro-rejuvenators, indicating that their addition helped soften the PAV-aged bitumen, promoting its diffusion through the cracked area during the healing process.

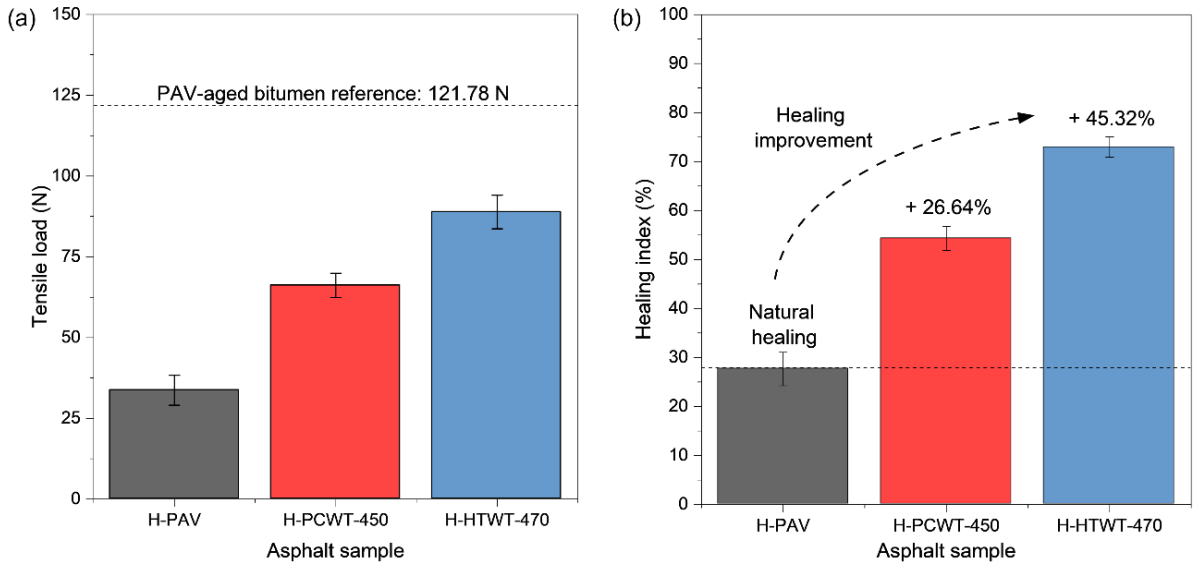

Figure 11. (a) Average results of tensile load at rupture for the PAV-aged bitumen before the healing process (reference line) and the healed PAV-aged samples without (H-PAV) and with the addition of optimized pyro-rejuvenators (H-PCWT-450 and H-HTWT-470); (b) Healing indices for the H-reference, H-PCWT-450, and H-HWTWT-470 samples.

Based on these results, it can be preliminarily concluded that the addition of pyro-rejuvenators positively impacted the recovery of the initial tensile force in PAV-aged bitumen. It is important to note that the tensile force recovery in the healed samples with pyro-rejuvenators can be attributed to a combined effect of the bitumen's natural intrinsic healing ability and the softening effect of the pyro-rejuvenators [11]. The contribution of each factor will be analyzed and discussed next.

To quantify the recovery in tensile force for each of the healed samples, Figure 11b shows the average healing indices (*HI*) for the H-PAV, H-PCWT-450, and H-HTWT-470 samples with values of 27.65%, 54.30%, and 72.98%, respectively. Overall, samples containing pyro-rejuvenators exhibited superior healing performance compared to the naturally healed samples,

consistent with the previously discussed tensile strength measurements. It should be noted that the HI values for the PAV-aged samples incorporating the pyro-rejuvenators provide an overall measure of the healing effect, which results from both the intrinsic self-healing of bitumen and the healing contributed by the softening effect of each pyro-rejuvenator. To separate and quantify each of these healing contributions, a Healing Index improvement (HI_i) was determined as shown by Equation 6:

$$HI_i(\%) = HI_R - HI_{PAV} \quad (6)$$

where the HI_{PAV} and HI_R are the healing indices for the PAV and PAV with pyro-rejuvenator addition, respectively.

The HI_i (%) values are displayed above each HI bar in Figure 11b, and these reaching +26.64% and +45.32% for H-PCWT-450 and H-HTWT-470, respectively. These values represent the healing provided by the pyro-rejuvenators, while the intrinsic self-healing is represented by a constant value of 27.65% (H-PAV). The healing effect of the pyro-rejuvenator is attributed to the high content of aromatics and alkenes, which aid in restoring the maltene fraction of the PAV-aged bitumen. These compounds promote the segregation of asphaltene structures, reducing their molecular interactions and enhancing their solubility within the bituminous matrix [23]. The resulting softening and improved stability of the asphalt matrix enhance adhesion between binder molecules, thereby promoting crack healing. Figure 11b shows that the PAV-aged sample with HTWT-470 exhibits the highest healing effect. This can be attributed to differences in the chemical composition of the pyro-rejuvenators, particularly the higher abundance of limonene and cymene in HTWT-470 (see Table S4 in supplementary materials). These compounds have strong solvent properties, which facilitate better softening of the aged asphalt during its intrinsic self-healing. In fact, Quezada et al. [71] demonstrated through molecular dynamics simulations that limonene and cymene from pyro-oils interact chemically with specific functional groups in asphalt binder molecules, promoting both diffusion and

softening of the bituminous matrix. Based on our results, it can be concluded that the addition of the HTWT-470 pyro-rejuvenator is the best option to promote self-healing in PAV-aged bituminous materials.

4. CONCLUSIONS

This study presents the design and synthesis of novel pyro-rejuvenators for enhancing asphalt self-healing, achieved through precise tuning of aromatic and alkene compositions in oils derived from the pyrolysis and subsequent distillation of waste tires (PCWT and HTWT). The efficacy of these pyro-rejuvenators was demonstrated by the restoration of tensile strength in PAV-aged bitumen samples exhibiting cracks. From these findings, we conclude the following:

- Thermogravimetric analysis (TGA/DTG) revealed that thermal degradation of both PCWT and HTWT proceeds through four distinct stages with comparable profiles. Notably, PCWT had a higher fraction of synthetic rubbers (butadiene rubber and styrene-butadiene rubber), whereas HTWT is enriched in natural rubber. These compositional differences correspond to the divergent mechanical performance demands inherent to each tire type.
- The chemical composition of pyro-oils was strongly influenced by the type of waste tire. Pyro-oils derived from PCWT exhibited a higher concentration of monoaromatics, whereas those from HTWT were predominantly composed of alkenes. The distinct composition and physical properties of these pyro-oils underscore their promising potential as effective rejuvenators for aged asphalt.
- Application of response surface methodology (RSM) allowed for the optimization of production conditions to maximize the content of monoaromatics and alkenes in the pyro-rejuvenators. These compounds play a critical role in restoring the maltene-to-asphaltene balance disrupted by aging, thereby enhancing the self-healing capacity of aged asphalt.
- The combined pyrolysis–distillation process effectively enhanced the composition and

physical properties of oils derived from waste tires. The resulting pyro-rejuvenators exhibited low viscosity, enabling efficient penetration into microcracks within aged asphalt, while their rich aromatic and alkene content promoted improved self-healing performance.

- Incorporation of both pyro-rejuvenators enhanced the tensile strength of cracked PAV-aged bitumen, confirming their self-healing efficacy. Notably, the HTWT-470 pyro-rejuvenator exhibited a significantly greater healing effect than PCWT-450, likely attributable to its higher concentrations of limonene and cymene. These compounds, with strong solvent properties, may more effectively facilitate softening of the aged asphalt, thereby enhancing intrinsic self-healing.

In conclusion, precisely engineered pyro-rejuvenators from waste tires, optimized through pyrolysis and distillation, offer a sustainable route to both valorize waste and extend pavement service life. Our results highlight their potential to restore asphalt performance, yet the mechanistic interactions between active rejuvenating species and asphalt remain incompletely understood. Advancing this field will require integrated spectroscopic analyses, molecular modeling, and field validation to ensure long-term performance and environmental safety. Bridging these gaps is essential to transform laboratory insights into reliable, sustainable solutions for real-world asphalt infrastructure.

5. SUPPORTING INFORMATION

The supporting information accompanying this paper includes:

1. Calibration curves for toluene, limonene and cymene.
2. Spectral windows of 600 – 1200 cm^{-1} for FTIR-ATR of distillation cuts.
3. Effective carbon number calculations.
4. GC-MS characterization for pyro-oils and pyro-rejuvenator.

6. ACKNOWLEDGMENTS

The authors thank the financial support given by the National Research and Development Agency (ANID) through the Research Project FONDEF No. ID21I10127. The authors thank the technical staff of UDT, University of Concepción, for their support in producing and characterizing the waste tire pyrolytic oils.

7. REFERENCES

(1) World Bank. *Transitions at the Heart of the Climate Challenge*; 2021. https://www.worldbank.org/en/news/feature/2021/05/24/transitions-at-the-heart-of-the-climate-challenge. Accessed: 30-09-2025.

(2) Thives, L. P.; Ghisi, E. Asphalt Mixtures Emission and Energy Consumption: A Review. *Renewable and Sustainable Energy Reviews* **2017**, *72*, 473–484. https://doi.org/10.1016/J.RSER.2017.01.087.

(3) He, L.; Tao, M.; Liu, Z.; Cao, Z.; Zhu, J.; Gao, J.; bergh, W. Van den; Chailleux, E.; Huang, Y.; Vasconcelos, K.; Cannone Falchetto, A.; Balieu, R.; Grenfell, J.; Wilson, D. J.; Valentin, J.; Kowalski, K. J.; Rzek, L.; Gaspar, L.; Ling, T.; Ma, Y. Biomass Valorization toward Sustainable Asphalt Pavements: Progress and Prospects. *Waste Management* **2023**, *165*, 159–178. https://doi.org/10.1016/J.WASMAN.2023.03.035.

(4) Zeiada, W.; Liu, H.; Ezzat, H.; Al-Khateeb, G. G.; Shane Underwood, B.; Shanableh, A.; Samarai, M. Review of the Superpave Performance Grading System and Recent Developments in the Performance-Based Test Methods for Asphalt Binder Characterization. *Constr Build Mater* **2022**, *319*, 126063. https://doi.org/10.1016/J.CONBUILDMAT.2021.126063.

(5) Behnood, A. Application of Rejuvenators to Improve the Rheological and Mechanical Properties of Asphalt Binders and Mixtures: A Review. *J Clean Prod* **2019**, *231*, 171–182. https://doi.org/10.1016/J.JCLEPRO.2019.05.209.

(6) Ren, S.; Liu, X.; Lin, P.; Erkens, S.; Xiao, Y. Chemo-Physical Characterization and Molecular Dynamics Simulation of Long-Term Aging Behaviors of Bitumen. *Constr Build Mater* **2021**, *302*, 124437. https://doi.org/10.1016/J.CONBUILDMAT.2021.124437.

(7) Speight, J. G. Asphalt Chemistry. *Asphalt Materials Science and Technology* **2016**, 253–301. https://doi.org/10.1016/B978-0-12-800273-5.00006-4.

(8) Pipintakos, G.; Soenen, H.; Ching, H. Y. V.; Velde, C. Vande; Doorslaer, S. Van; Lemière, F.; Varveri, A.; Van den bergh, W. Exploring the Oxidative Mechanisms of Bitumen after Laboratory Short- and Long-Term Ageing. *Constr Build Mater* **2021**, *289*, 123182. https://doi.org/10.1016/J.CONBUILDMAT.2021.123182.

(9) Wang, Y.; Wang, W.; Wang, L. Understanding the Relationships between Rheology and Chemistry of Asphalt Binders: A Review. *Constr Build Mater* **2022**, *329*, 127161. https://doi.org/10.1016/J.CONBUILDMAT.2022.127161.

(10) Schwettmann, K.; Nytus, N.; Weigel, S.; Radenberg, M.; Stephan, D. Effects of Rejuvenators on Bitumen Ageing during Simulated Cyclic Reuse: A Review. *Resour Conserv Recycl* **2023**, *190*, 106776. https://doi.org/10.1016/J.RESCONREC.2022.106776.

(11) Chávez-Delgado, M.; Colina, J. R.; Segura, C.; Álvarez, C.; Osorio-Vargas, P.; Arteaga-Pérez, L. E.; Norambuena-Contreras, J. Asphalt Pyro-Rejuvenators Based on Waste Tyres: An Approach to Improve the Rheological and Self-Healing Properties of Aged Binders. *J Clean Prod* **2024**, *452*, 142179. https://doi.org/10.1016/J.JCLEPRO.2024.142179.

(12) Baghaee Moghaddam, T.; Baaj, H. The Use of Rejuvenating Agents in Production of Recycled Hot Mix Asphalt: A Systematic Review. *Constr Build Mater* **2016**, *114*, 805–816. https://doi.org/10.1016/J.CONBUILDMAT.2016.04.015.

(13) Alfe, M.; Gargiulo, V.; Ruoppolo, G.; Cammarota, F.; Calandra, P.; Oliviero Rossi, C.; Loise, V.; Porto, M.; Di Capua, R.; Caputo, P. Microstructural Modifications in Bitumens Rejuvenated by Oil from Pyrolysis of Waste Tires. *Front Chem* **2024**, *12*, 1512905. https://doi.org/10.3389/FCHEM.2024.1512905/BIBTEX.

(14) Hung, A. M.; Li, M.; Wu, G.; Fini, E. H. Effects of Liquefied Waste Plastics on Chemical and Rheological Properties of Bitumen. *Journal of Transportation Engineering, Part B: Pavements* **2023**, *149* (2), 04023003. https://doi.org/10.1061/JPEODX.PVENG-1153;PAGEGROUP:STRING:PUBLICATION.

(15) Yan, S.; Dong, Q.; Chen, X.; Zhou, C.; Dong, S.; Gu, X. Application of Waste Oil in Asphalt Rejuvenation and Modification: A Comprehensive Review. *Constr Build Mater* **2022**, *340*, 127784. https://doi.org/10.1016/J.CONBUILDMAT.2022.127784.

(16) Arafat, S.; Wasiuddin, N. M.; Mohammad, L. N. Evaluation of Bio-Based and Petroleum-Based Rejuvenator Based on Cracking Susceptibility of Hot Mix Asphalt with High RAP Content. *Constr Build Mater* **2023**, *371*, 130725. https://doi.org/10.1016/J.CONBUILDMAT.2023.130725.

(17) Al-Saffar, Z. H.; Yaacob, H.; Satar, M. K. I. M.; Kamarudin, S. N. N.; Mahmud, M. Z. H.; Ismail, C. R.; Hassan, S. A.; Mashros, N. A Review on the Usage of Waste Engine Oil with Aged Asphalt as a Rejuvenating Agent. *Mater Today Proc* **2021**, *42*, 2374–2380. https://doi.org/10.1016/J.MATPR.2020.12.330.

(18) Wang, J.; Lv, S.; Liu, J.; Peng, X.; Lu, W.; Wang, Z.; Xie, N. Performance Evaluation of Aged Asphalt Rejuvenated with Various Bio-Oils Based on Rheological Property Index. *J Clean Prod* **2023**, *385*, 135593. https://doi.org/10.1016/J.JCLEPRO.2022.135593.

(19) Fang, Y.; Zhang, Z.; Yang, J.; Li, X. Comprehensive Review on the Application of Bio-Rejuvenator in the Regeneration of Waste Asphalt Materials. *Constr Build Mater* **2021**, *295*, 123631. https://doi.org/10.1016/J.CONBUILDMAT.2021.123631.

(20) Rahman, M. M.; Yu, Y.; Wu, H. Valorisation of Waste Tyre via Pyrolysis: Advances and Perspectives. *Energy and Fuels* **2022**, *36* (20), 12429–12474. https://doi.org/10.1021/ACS.ENERGYFUELS.2C02053/ASSET/IMAGES/LARGE/EF2C02053_0036.JPEG.

(21) Formela, K. Waste Tire Rubber-Based Materials: Processing, Performance Properties and Development Strategies. *Advanced Industrial and Engineering Polymer Research* **2022**, *5* (4), 234–247. https://doi.org/10.1016/J.AIEPR.2022.06.003.

(22) Kumar, A.; Choudhary, R.; Kumar, A. Evaluation of Waste Tire Pyrolytic Oil as a Rejuvenation Agent for Unmodified, Polymer-Modified, and Rubber-Modified Aged Asphalt Binders. *Journal of Materials in Civil Engineering* **2022**, *34* (10), 04022246. https://doi.org/10.1061/(ASCE)MT.1943-5533.0004400.

(23) Chávez-Delgado, M.; Concha, J. L.; Caro, S.; Silva, C. P.; Arteaga-Pérez, L. E.; Norambuena-Contreras, J. Self-Healing Asphalt with Optimised Tyre-Based Pyro-Rejuvenator. *Fuel* **2025**, *400*, 135747. https://doi.org/10.1016/J.FUEL.2025.135747.

(24) Delgadillo, R.; González, A.; Marzal, I.; Concha, J. L.; Segura, C.; Arteaga-Pérez, L. E.; Norambuena-Contreras, J. Rheological and Chemical Effects of Waste Tire Pyrolytic Oil and Its Encapsulation as Rejuvenators on Asphalt Binders. *Polymers 2025, Vol. 17, Page 2449* **2025**, *17* (18), 2449. https://doi.org/10.3390/POLYM17182449.

(25) Norambuena-Contreras, J.; Arteaga-Pérez, L. E.; Concha, J. L.; Gonzalez-Torre, I. Pyrolytic Oil from Waste Tyres as a Promising Encapsulated Rejuvenator for the Extrinsic Self-Healing of Bituminous Materials. *Road Materials and Pavement Design* **2021**, *22* (sup1), S117–S133. https://doi.org/10.1080/14680629.2021.1907216.

(26) Li, C.; Rajib, A.; Sarker, M.; Liu, R.; Fini, E. H.; Cai, J. Balancing the Aromatic and Ketone Content of Bio-Oils as Rejuvenators to Enhance Their Efficacy in Restoring Properties of Aged Bitumen. *ACS Sustain Chem Eng* **2021**, *9* (20), 6912–6922. https://doi.org/10.1021/ACSSUSCHEMENG.0C09131/SUPPL_FILE/SC0C09131_SI_001.PDF.

(27) Campuzano, F.; Abdul Jameel, A. G.; Zhang, W.; Emwas, A. H.; Agudelo, A. F.; Martínez, J. D.; Sarathy, S. M. On the Distillation of Waste Tire Pyrolysis Oil: A Structural Characterization of the Derived Fractions. *Fuel* **2021**, *290* (August 2020). https://doi.org/10.1016/j.fuel.2020.120041.

(28) Chávez-Delgado, M.; Concha, J. L.; Caro, S.; Arteaga-Pérez, L. E.; Norambuena-Contreras, J. Enhancing Rheological and Self-Healing Properties of Aged Bitumen Using a Pyro-Rejuvenator from Waste Tyres. *Constr Build Mater* **2025**, *470*, 140639. https://doi.org/10.1016/J.CONBUILDMAT.2025.140639.

(29) *D2872 Standard Test Method for Effect of Heat and Air on a Moving Film of Asphalt Binder (Rolling Thin-Film Oven Test)*. https://www.astm.org/d2872-22.html (accessed 2024-10-01).

(30) 6521-19, A. D. Standard Practice for Accelerated Aging of Asphalt Binder Using a Pressurised Aging Vessel (PAV). ASTM International 2019. https://doi.org/https://doi.org/10.1520/D6521-19.

(31) *D529 Standard Practice for Enclosed Carbon-Arc Exposures of Bituminous Materials*. https://www.astm.org/d0529-00.html (accessed 2024-10-01).

(32) D3172-89, A. Standard Practice for Proximate Analysis of Coal and Coke. 2013.

(33) *D86 Standard Test Method for Distillation of Petroleum Products and Liquid Fuels at Atmospheric Pressure*. https://www.astm.org/d0086-23ae01.html (accessed 2024-10-01).

(34) Menares, T.; Herrera, J.; Romero, R.; Osorio, P.; Arteaga-Pérez, L. E. Waste Tires Pyrolysis Kinetics and Reaction Mechanisms Explained by TGA and Py-GC/MS under Kinetically-Controlled Regime. *Waste Management* **2020**, *102*, 21–29. https://doi.org/10.1016/J.WASMAN.2019.10.027.

(35) Hofko, B.; Alavi, M. Z.; Grothe, H.; Jones, D.; Harvey, J. Repeatability and Sensitivity of FTIR ATR Spectral Analysis Methods for Bituminous Binders. *Materials and Structures/Materiaux et Constructions* **2017**, *50* (3), 1–15. https://doi.org/10.1617/s11527-017-1059-x.

(36) Szulejko, J. E.; Kim, K. H. Re-Evaluation of Effective Carbon Number (ECN) Approach to Predict Response Factors of 'Compounds Lacking Authentic Standards or Surrogates' (CLASS) by Thermal Desorption Analysis with GC–MS. *Anal Chim Acta* **2014**, *851* (C), 14–22. https://doi.org/10.1016/J.ACA.2014.08.033.

(37) Kim, Y. H.; Kim, K. H.; Szulejko, J. E.; Bae, M. S.; Brown, R. J. C. Experimental Validation of an Effective Carbon Number-Based Approach for the Gas Chromatography–Mass Spectrometry Quantification of 'Compounds Lacking Authentic Standards or Surrogates.' *Anal Chim Acta* **2014**, *830*, 32–41. https://doi.org/10.1016/J.ACA.2014.04.052.

(38) Mkhize, N. M.; van der Gryp, P.; Danon, B.; Görgens, J. F. Effect of Temperature and Heating Rate on Limonene Production from Waste Tyre Pyrolysis. *J Anal Appl Pyrolysis* **2016**, *120*, 314–320. https://doi.org/10.1016/j.jaap.2016.04.019.

(39) Williams, P. T. Pyrolysis of Waste Tyres: A Review. *Waste Management* **2013**, *33* (8), 1714–1728. https://doi.org/10.1016/j.wasman.2013.05.003.

(40) Martínez, J. D.; Puy, N.; Murillo, R.; García, T.; Navarro, M. V.; Mastral, A. M. Waste Tyre Pyrolysis – A Review. *Renewable and Sustainable Energy Reviews* **2013**, *23*, 179–213. https://doi.org/10.1016/J.RSER.2013.02.038.

(41) Han, Z.; Cong, P.; Qiu, J. Microscopic Experimental and Numerical Research on Rejuvenators: A Review. *Journal of Traffic and Transportation Engineering (English Edition)* **2022**, *9* (2), 180–207. https://doi.org/10.1016/J.JTTE.2022.01.002.

(42) ASTM. *D113-17 Standard Test Method for Ductility of Asphalt Materials*; 2023; Vol. 04.03. https://doi.org/10.1520/D0113_D0113-17R23E01.

(43) Osorio-Vargas, P.; Menares, T.; Lick, I. D.; Casella, M. L.; Romero, R.; Jiménez, R.; Arteaga-Pérez, L. E. Tuning the Product Distribution during the Catalytic Pyrolysis of Waste Tires: The Effect of the Nature of Metals and the Reaction Temperature. *Catal Today* **2021**, *372* (April 2020), 164–174. https://doi.org/10.1016/j.cattod.2020.10.035.

(44) Gao, N.; Wang, F.; Quan, C.; Santamaria, L.; Lopez, G.; Williams, P. T. Tire Pyrolysis Char: Processes, Properties, Upgrading and Applications. *Prog Energy Combust Sci* **2022**, *93*, 101022. https://doi.org/10.1016/J.PECS.2022.101022.

(45) Jiang, G.; Pan, J.; Deng, W.; Sun, Y.; Guo, J.; Che, K.; Yang, Y.; Lin, Z.; Sun, Y.; Huang, C.; Zhang, T. Recovery of High Pure Pyrolytic Carbon Black from Waste Tires by Dual Acid Treatment. *J Clean Prod* **2022**, *374*, 133893. https://doi.org/10.1016/J.JCLEPRO.2022.133893.

(46) Osorio-Vargas, P.; Lick, I. D.; Pizzio, L. R.; Alejandro, S.; Casas-Ledón, Y.; Poblete, J.; Casella, M. L.; Arteaga-Pérez, L. E. Using Tungstophosphoric Acid-Modified CeO2, TiO2, and SiO2 Catalysts to Promote Secondary Reactions Leading to Aromatics during Waste Tire Pyrolysis. *Molecular Catalysis* **2022**, *531*, 112682. https://doi.org/10.1016/J.MCAT.2022.112682.

(47) Zheng, D.; Cheng, J.; Dai, C.; Xu, R.; Wang, X.; Liu, N.; Wang, N.; Yu, G.; Chen, B. Study of Passenger-Car-Waste-Tire Pyrolysis: Behavior and Mechanism under Kinetical Regime. *Waste Management* **2022**, *148*, 71–82. https://doi.org/10.1016/J.WASMAN.2022.05.024.

(48) Rijo, B.; Soares Dias, A. P.; Wojnicki, Ł. Catalyzed Pyrolysis of Scrap Tires Rubber. *J Environ Chem Eng* **2022**, *10* (1), 107037. https://doi.org/10.1016/J.JECE.2021.107037.

(49) Rijo, B.; Soares Dias, A. P.; Wojnicki, Ł. Catalyzed Pyrolysis of Scrap Tires Rubber. *J Environ Chem Eng* **2022**, *10* (1), 107037. https://doi.org/10.1016/J.JECE.2021.107037.

(50) Danon, B.; Görgens, J. Determining Rubber Composition of Waste Tyres Using Devolatilisation Kinetics. *Thermochim Acta* **2015**, *621*, 56–60. https://doi.org/10.1016/j.tca.2015.10.008.

(51) Danon, B.; Mkhize, N. M.; Van Der Gryp, P.; Görgens, J. F. Combined Model-Free and Model-Based Devolatilisation Kinetics of Tyre Rubbers. *Thermochim Acta* **2015**, *601*, 45–53. https://doi.org/10.1016/j.tca.2014.12.003.

(52) Lopez, G.; Olazar, M.; Amutio, M.; Aguado, R.; Bilbao, J. Influence of Tire Formulation on the Products of Continuous Pyrolysis in a Conical Spouted Bed Reactor. *Energy & Fuels* **2009**, *23* (11), 5423–5431. https://doi.org/10.1021/ef900582k.

(53) Campuzano, F.; Martínez, J. D.; Santamaría, A. F. A.; Sarathy, S. M.; Roberts, W. L. Pursuing the End-of-Life Tire Circularity: An Outlook toward the Production of Secondary Raw Materials from Tire Pyrolysis Oil. *Energy & Fuels* **2023**, *37* (13), 8836–8866. https://doi.org/10.1021/ACS.ENERGYFUELS.3C00847.

(54) Sanchís, A.; Veses, A.; Martínez, J. D.; López, J. M.; García, T.; Murillo, R. The Role of Temperature Profile during the Pyrolysis of End-of-Life-Tyres in an Industrially Relevant Conditions Auger Plant. *J Environ Manage* **2022**, *317*, 115323. https://doi.org/https://doi.org/10.1016/j.jenvman.2022.115323.

(55) Qi, J.; Hu, M.; Xu, P.; Zhu, F.; Yuan, H.; Wang, Y.; Chen, Y. Study on Pyrolysis of Waste Tires and Condensation Characteristics of Products in a Pilot Scale Screw-Propelled Reactor. *Fuel* **2023**, *353*, 129225. https://doi.org/10.1016/J.FUEL.2023.129225.

(56) Taleb, D. A.; Hamid, H. A.; Deris, R. R. R.; Zulkifli, M.; Khalil, N. A.; Ahmad Yahaya, A. N. Insights into Pyrolysis of Waste Tire in Fixed Bed Reactor: Thermal Behavior. *Mater Today Proc* **2020**, *31* (February), 178–186. https://doi.org/10.1016/j.matpr.2020.01.569.

(57) Banar, M.; Akyildiz, V.; Özkan, A.; Çokaygil, Z.; Onay, Ö. Characterization of Pyrolytic Oil Obtained from Pyrolysis of TDF (Tire Derived Fuel). *Energy Convers Manag* **2012**, *62*, 22–30. https://doi.org/10.1016/j.enconman.2012.03.019.

(58) Akkouche, N.; Balistrou, M.; Loubar, K.; Awad, S.; Tazerout, M. Heating Rate Effects on Pyrolytic Vapors from Scrap Truck Tires. *J Anal Appl Pyrolysis* **2017**, *123*, 419–429. https://doi.org/10.1016/j.jaap.2016.10.005.

(59) Rofiqul Islam, M.; Haniu, H.; Rafiqul Alam Beg, M. Liquid Fuels and Chemicals from Pyrolysis of Motorcycle Tire Waste: Product Yields, Compositions and Related Properties. *Fuel* **2008**, *87* (13–14), 3112–3122. https://doi.org/10.1016/J.FUEL.2008.04.036.

(60) Pyshyev, S.; Lypko, Y.; Chervinskyy, T.; Fedevych, O.; Kułażyński, M.; Pstrowska, K. Application of Tyre Derived Pyrolysis Oil as a Fuel Component. *S Afr J Chem Eng* **2023**, *43*, 342–347. https://doi.org/10.1016/J.SAJCE.2022.12.003.

(61) Ucar, S.; Karagoz, S.; Ozkan, A. R.; Yanik, J. Evaluation of Two Different Scrap Tires as Hydrocarbon Source by Pyrolysis. *Fuel* **2005**, *84* (14–15), 1884–1892. https://doi.org/10.1016/j.fuel.2005.04.002.

(62) Singh, R. K.; Ruj, B.; Jana, A.; Mondal, S.; Jana, B.; Sadhukhan, A. K.; Gupta, P. Pyrolysis of Three Different Categories of Automotive Tyre Wastes: Product Yield Analysis and Characterization. *J. Anal. Appl. Pyrolysis* **2018**, *135*, 379–389.

(63) Zheng, D.; Cheng, J.; Dai, C.; Xu, R.; Wang, X.; Liu, N.; Wang, N.; Yu, G.; Chen, B. Study of Passenger-Car-Waste-Tire Pyrolysis: Behavior and Mechanism under Kinetical

Regime. *Waste Management* **2022**, *148*, 71–82. https://doi.org/10.1016/J.WASMAN.2022.05.024.

(64) Danon, B.; Van Der Gryp, P.; Schwarz, C. E.; Görgens, J. F. A Review of Dipentene (Dl-Limonene) Production from Waste Tire Pyrolysis. *J Anal Appl Pyrolysis* **2015**, *112*, 1–13. https://doi.org/10.1016/j.jaap.2014.12.025.

(65) Januszewicz, K.; Kazimierski, P.; Kosakowski, W.; Lewandowski, W. M. Waste Tyres Pyrolysis for Obtaining Limonene. *Materials* **2020**, *13* (1359), 1–30. https://doi.org/10.3390/MA13061359.

(66) Ye, W.; Xu, X.; Zhan, M.; Huang, Q.; Li, X.; Jiao, W.; Yin, Y. Formation Behavior of PAHs during Pyrolysis of Waste Tires. *J Hazard Mater* **2022**, *435* (128997), 1–11. https://doi.org/10.1016/J.JHAZMAT.2022.128997.

(67) Laresgoiti, M. F.; Caballero, B. M.; De Marco, I.; Torres, A.; Cabrero, M. A.; Chomón, M. J. Characterization of the Liquid Products Obtained in Tyre Pyrolysis. *J Anal Appl Pyrolysis* **2004**, *71* (2), 917–934. https://doi.org/10.1016/j.jaap.2003.12.003.

(68) Lopez, G.; Alvarez, J.; Amutio, M.; Mkhize, N. M.; Danon, B.; van der Gryp, P.; Görgens, J. F.; Bilbao, J.; Olazar, M. Waste Truck-Tyre Processing by Flash Pyrolysis in a Conical Spouted Bed Reactor. *Energy Convers Manag* **2017**, *142*, 523–532. https://doi.org/10.1016/J.ENCONMAN.2017.03.051.

(69) Mikulski, M.; Ambrosewicz-Walacik, M.; Hunicz, J.; Nitkiewicz, S. Combustion Engine Applications of Waste Tyre Pyrolytic Oil. *Prog Energy Combust Sci* **2021**, *85*, 100915. https://doi.org/10.1016/J.PECS.2021.100915.

(70) Luo, S.; Feng, Y. The Production of Fuel Oil and Combustible Gas by Catalytic Pyrolysis of Waste Tire Using Waste Heat of Blast-Furnace Slag. *Energy Convers Manag* **2017**, *136*, 27–35. https://doi.org/10.1016/J.ENCONMAN.2016.12.076.

(71) Quezada, G. R.; Solar, C.; Saavedra, J. H.; Petit, K.; Martin-Martínez, F. J.; Arteaga-Pérez, L. E.; Norambuena-Contreras, J. Operando FTIR-ATR with Molecular Dynamic Simulations to Understand the Diffusion Mechanism of Waste Tire-Derived Pyrolytic Oil for Asphalt Self-Healing. *Fuel* **2024**, *357*, 129834. https://doi.org/10.1016/J.FUEL.2023.129834.

(72) Sarjono, P. R.; Ismiyarto; Ngadiwiyana; Adiwibawa Prasetya, N. B.; Rosydhaulfa; Ariestiani, B.; Kusuma, A. B.; Darmastuti, N. E.; Rohman, J. H. F. Antioxidant Activity from Limonene Encapsulated by Chitosan. *IOP Conf Ser Mater Sci Eng* **2019**, *509* (1), 012113. https://doi.org/10.1088/1757-899X/509/1/012113.

(73) De Oliveira, T. M.; De Carvalho, R. B. F.; Da Costa, I. H. F.; De Oliveira, G. A. L.; De Souza, A. A.; De Lima, S. G.; De Freitas, R. M. Evaluation of P-Cymene, a Natural Antioxidant. *Pharm Biol* **2015**, *53* (3), 423–428. https://doi.org/10.3109/13880209.2014.923003.

(74) Martín-Luengo, M. A.; Yates, M.; Martínez Domingo, M. J.; Casal, B.; Iglesias, M.; Esteban, M.; Ruiz-Hitzky, E. Synthesis of P-Cymene from Limonene, a Renewable Feedstock. *Appl Catal B* **2008**, *81* (3–4), 218–224. https://doi.org/10.1016/j.apcatb.2007.12.003.

(75) Satira, A.; Espro, C.; Paone, E.; Calabrò, P. S.; Pagliaro, M.; Ciriminna, R.; Mauriello, F. The Limonene Biorefinery: From Extractive Technologies to Its Catalytic Upgrading into p-Cymene. *Catalysts 2021, Vol. 11, Page 387* **2021**, *11* (3), 387. https://doi.org/10.3390/CATAL11030387.

(76) Martínez, J. D.; Campuzano, F.; Agudelo, A. F.; Cardona-Uribe, N.; Arenas, C. N. Chemical Recycling of End-of-Life Tires by Intermediate Pyrolysis Using a Twin-Auger Reactor: Validation in a Laboratory Environment. *J Anal Appl Pyrolysis* **2021**, *159* (105298), 1–11. https://doi.org/10.1016/j.jaap.2021.105298.

(77) Faizi, N.; Alvi, Y. Statistical Tests of Significance. *Biostatistics Manual for Health Research* **2023**, 45–62. https://doi.org/10.1016/B978-0-443-18550-2.00009-8.

(78) Alzahrani, N.; Nahil, M. A.; Williams, P. T. Co-Pyrolysis of Waste Plastics and Tires: Influence of Interaction on Product Oil and Gas Composition. *Journal of the Energy Institute* **2025**, *118*, 101908. https://doi.org/10.1016/J.JOEI.2024.101908.

Graphical Abstract